Precision Agric
DOI 10.1007/s11119-012-9283-4

Evaluation of spectral indices and continuous wavelet analysis to quantify aphid infestation in wheat

Juhua Luo · Wenjiang Huang · Lin Yuan · Chunjiang Zhao · Shizhou Du · Jingcheng Zhang · Jinling Zhao

Abstract Wheat aphid, *Sitobion avenae F.* is one of the most destructive insects infesting winter wheat and appears almost annually in northwest China. Past studies have demonstrated the potential of remote sensing for detecting crop diseases and insect damage. This study aimed to investigate the spectroscopic estimation of leaf aphid density by applying continuous wavelet analysis to the reflectance spectra (350–2 500 nm) of 60 winter wheat leaf samples. Continuous wavelet transform (CWT) was performed on each of the reflectance spectra to generate a wavelet power scalogram compiled as a function of wavelength location and scale of decomposition. Linear regression between the wavelet power and aphid density was to identify wavelet features (coefficients) that might be the most sensitive to aphid density. The results identified five wavelet features between 350 and 2 500 nm that provided strong correlations with leaf aphid density. Spectral indices commonly used to monitor crop stresses were also employed to estimate aphid density. Multivariate linear regression models based on six sensitivity spectral indices or five wavelet features were established to estimate aphid density. The results showed that the model with five wavelet features ($R^2 = 0.72$, RMSE = 16.87) performed better than the model with six sensitivity spectral indices ($R^2 = 0.56$, RMSE = 21.19), suggesting that the spectral features extracted through CWT might potentially reflect aphid density. The results also provided a new method for estimating aphid density using remote sensing.

J. Luo
State Key Laboratory of Lake Science and Environment, Nanjing Institute of Geography and Limnology, Chinese Academy of Sciences, Nanjing, China

W. Huang (✉)
Center for Earth Observation and Digital Earth, Chinese Academy of Sciences, Beijing, China
e-mail: yellowstar0618@163.com

L. Yuan · C. Zhao · J. Zhang · J. Zhao
Beijing Research Center for Information Technology in Agriculture, Beijing, China

S. Du
Institute of Crops Anhui Academy of Agricultural Sciences, Hefei, China

Published online: 22 September 2012

Keywords Winter wheat · Aphid density · Spectral indices · Continuous wavelet analysis · Hyperspectral remote sensing

Introduction

Wheat aphid, *Sitobion avenae (Fabricius)*, is one of the most destructive pests in agricultural systems, especially in the regions of temperate climate in the northern and southern hemispheres and occurs annually in the wheat planting area of China. Aphid feed on wheat plants and injects saliva that contains plant toxins, which results in significant yield loss (Rabbinge et al. 1981; Halbert et al. 1992). It is reported that the threshold of wheat aphid infestation that indicates when management action should be triggered is considered to be on average 5 per tiller. It has been reported that aphid density has a positive correlation with leaf damage and yield (Luo et al. 2011). It has also been shown that a density of 10 aphids per tiller results in a 7 % yield loss and 40 aphids per tiller leads to an 11 % yield loss (Shaoyou et al. 1986; Larsson 2005).

Pesticide applications are effective in controlling aphid and minimizing the yield loss of winter wheat (Fluckiger et al. 1992; Pike et al. 1993) but they are not always effective and economical for long-term control (Lyda and Burnett 1970; Rush and Lyda 1982; Whitson and Hine 1986). This is because the automatic spray systems tend to use excessive amounts of pesticide due to lacking the irregular infestation patterns, which not only increases costs of production but also impacts on the environment (Higley and Pedigo 1993; Pimentel 1995; Ahmed et al. 2001). Therefore, in practice, it is important to monitor aphid infestation at critical junctures of crop growth and obtain spatial distribution information on aphid infestation within a particular field for site-specific management and judicious application of pesticides.

The common and conventional ways to obtain information of density infestation in the field is by manual field scouting, which has been shown to be expensive, time-consuming, and difficult for large farms (Zhang et al., 2003). However, hyperspectral remote sensing technology may be a superior alternative for obtaining spatial distribution information on aphid infestation density over a large area due to the relatively lower cost and the possibility for it to be mounted on airborne and space-borne platforms.

There has been some progress made in detecting aphid infestation density using hyperspectral remote sensing. Riedell and Blackmer (1999) reported that leaf reflectance in the 625–635 and 680–695 nm ranges, as well as the normalised total pigment to chlorophyll 'a' ratio index (NPCI) were good indicators of chlorophyll loss and leaf senescence caused by Russian wheat aphid (*Diuraphis noxia Kurdjumov*) and greenbug (*Schizaphis graminum Rondani*) feeding on wheat. Yang et al. (2005) used a hand-held radiometer in greenhouse experiments to characterise greenbug stress in wheat and found that the band centered at 694 nm and the vegetation indices derived from bands centered at 800 and 694 nm were the most sensitive to greenbug-damaged wheat. Mirik et al. (2006a) studied the relationship between spectral indices and greenbug abundance and found that damage sensitive spectral index1(DSSI1), damage sensitive spectral index2 (DSSI2), simple ratio (SR) and normalised difference vegetation index (NDVI) were related to damage by greenbug. Mirik et al. (2006b) developed an aphid index (AI) and found that AI had the strongest relationships with greenbug density. Mirik et al. (2007) found that remote sensing data had the potential to distinguish damage by Russian wheat aphid and quantify its abundance in wheat, but success for Russian wheat aphid density estimation depended on the selection of the spectral vegetation indices. Yang et al. (2009) suggested that

ratio-based vegetation indices (based on 800/450 and 950/450 nm) were useful in differentiating the stress caused by Russian wheat aphid and greenbug in wheat. These findings suggest that remote sensing using spectral reflectance and indices can be an effective technique for nondestructively detecting plants stressed by Russian wheat aphid and greenbug. However, practical applications of remote sensing methods using vegetation indices are limited because they employ only a limited number of spectral or hyperspectral bands, from which it is difficult to detect the subtle signals and spectral changes caused by aphid infestation.

Various physiological and biochemical factors, such as pigments, nutrient content and leaf water content, which can influence the tissue optical properties, change with wheat aphid infestation and thus affect the spectral response (Broge and Mortensen 2002; Sims and Gamon 2002; Ayala-Silva and Beyl 2005). Continuous wavelet analysis (CWA) has been reported as an emerging and potential tool for deriving biochemical constituent concentrations from leaf reflectance spectra (Blackburn 2007; Blackburn and Ferwerda 2008; Cheng et al. 2010). The continuous wavelet transform decomposes leaf reflectance spectra into a number of scale components so that each component is directly comparable with the reflectance spectra. Continuous wavelet analysis is used in this study as a spectral feature analysis tool to extract wavelet features (coefficients) that are sensitive to wheat aphid density. This study sought to answer two questions: (1) Is CWT more effective than the commonly used spectral indices for detecting aphid damage and estimating aphid density? (2) What are the most informative wavelet features for estimating aphid density?

Materials and methods

Leaf sample collection

Many wheat plants were collected at the grain filling stage, based on different aphid densities on the second leaves in an experimental field in Beijing Academy of Agriculture and Forestry Sciences, China (39°56′ N, 116°16′ E) on May 26, 2010. The plants were transported to the laboratory, and a total of 60 second leaves infested by wheat aphid were removed with scissors. They represented different aphid densities, ranging from 0 to 120 per leaf. Aphid numbers were counted and then they were removed before performing the spectral measurement.

Leaf spectral measurement

Leaf spectra were measured immediately after the aphid removal. Reflectance measurements of these sample leaves were recorded between 350 and 2 500 nm using a Fieldspec FR spectroradiometer (ASD Inc., Boulder, CO, USA) together with a leaf clip. This instrument sampled every 3 nm between 350 and 1 050 nm, and every 10 nm between 1 050 and 2 500 nm. Five reflectance spectra were taken per leaf using an ASD leaf clip covering a halogen bulb-illuminated area with a radius totaling 10 mm. A mean reflectance spectrum was calculated for each leaf.

Spectral indices

Table 1 represents 14 vegetation indices tested in this study for their sensitivity to aphid damage.

Table 1 Various vegetation indices compiled from literature

Spectral Index	Formula	References
Photochemical Reflectance Index (PRI)	$(R_{531} - R_{570})/(R_{531} + R_{570})$	Gamon et al. (1997)
Modified Chlorophyll Absorption Reflectance Index (MCARI)	$[(R_{700} - R_{670}) - 0.2(R_{700} - R_{550})] * (R_{700}/R_{670})$	Daughtry et al. (2000)
Aphid Index(AI)	$(R_{740} - R_{887})/(R_{691} - R_{698})$	Mirik et al. (2006a)
Triangular Vegetation Index (TVI)	$0.5[120(R_{750} - R_{550}) - 200(R_{670} - R_{550})]$	Broge and Leblanc (2001)
Damage Sensitive Spectral Index1 (DSSI1)	$(R_{719} - R_{873} - R_{509} - R_{537})/(R_{719} - R_{873} + R_{509} - R_{537})$	Mirik et al. (2006b)
Anthocuanin Reflectance Index (ARI)	$(R_{550})^{-1} - (R_{700})^{-1}$	Gitelson et al. (2001)
Narrow-band Normalised Difference Vegetation Index (NBNDVI)	$(R_{850} - R_{680})/(R_{850} + R_{680})$	Thenkabail et al. (2000)
Nitrogen Reflectance Index (NRI)	$(R_{570} - R_{670})/(R_{570} + R_{670})$	Filella et al. (1995)
Damage Sensitive Spectral Index2 (DSSI2)	$(R_{747} - R_{901} - R_{537} - R_{572})/(R_{747} - R_{901} + R_{537} - R_{572})$	Mirik et al. (2006a)
Plant Senescence Reflectance Index (PSRI)	$(R_{680} - R_{500})/R_{750}$	Merzlyak et al. (1999)
Structure Insensitive Pigment Index (SIPI)	$(R_{800} - R_{450})/(R_{800} - R_{680})$	Peñuelas and Inoue (1999)
Normalized Total Pigment to Chlorophyll a Ratio Index (NPCI)	$(R_{680} - R_{430})/(R_{680} - R_{430})$	Riedell and Blackmer (1999)
Plants Senescence Reflectance Index (PSRI)	$(R_{680} - R_{500})/R_{750}$	Merzlyak et al. (1999)
Normalized Difference Water Index (NDWI)	$(R_{860} - R_{1240})/(R_{860} + R_{1240})$	Gao (1996)

Continuous wavelet transformation (CWT)

Wavelet transform uses a mother wavelet basis function to convert the original reflectance spectrum into a set of coefficients. The main equation of wavelet transformation can be as follows:

$$\psi_{a,b}(\lambda) = \frac{1}{\sqrt{a}}\psi\left(\frac{\lambda - b}{a}\right) \tag{1}$$

where a is the scaling factor determining the width of the wavelet, b is the shifting factor indicating the position, $\psi_{a,b}(\lambda)$ represents the wavelets that are transformed by scaling and shifting the mother wavelet $\psi(\lambda)$.

In the transformation process, the output of CWT is given by Mallat (1991):

$$W_f(a,b) = \left(f, \psi_{a,b}\right) = \int_{+\infty}^{-\infty} f(\lambda)\psi_{a,b}(\lambda)d\lambda \tag{2}$$

where $f(\lambda)$ ($\lambda = 1, 2,\ldots,$n, n is the number of wavebands and herein n = 2151) is the reflectance spectrum and the coefficients ($W_f(a_i, b_j)$, i = 1, 2,…, m, j = 1, 2,…, n) are able to constitute a 2-dimensional scalogram (i.e., an m × n matrix), in which one dimension is scale and the other is wavelength. The value of each element of the scalogram represents the wavelet power that indicates the correlation between the scaled and shifted mother

wavelet and a segment of the reflectance spectrum. Spectral signals can vary in both amplitude (e.g. feature depth) and scale (e.g., feature width). Each capturing spectral features of different widths by CWT were as scales. Narrow absorption features in the original spectrum will be captured by wavelets at a low scale (narrow width), whilst the shape of the continuum will be captured by wavelets at a higher scale (Blackburn and Ferwerda 2008; Rivard et al. 2008).

It has been reported that the shape of the absorption features of vegetation was similar to a Gaussian or quasi-Gaussian function (Torrence and Compo 1998). Therefore, the second derivative of Gaussian (DOG) also known as the Mexican Hat was used as the mother wavelet basis (Muraki 1995; Torrence and Compo 1998; Cheng et al. 2011). In this study, the leaf reflectance spectra ranged from 350 to 2 500 nm and there were 2 151 bands available (350–2 500 nm). Any scale greater than $2^{10} = 1024$ was discarded because the decomposed components at high scales did not carry meaningful spectral information. All CWT operations were carried out by Matlab 7.1 (Natick, MA, USA).

Calibration and validation of regression models

The entire dataset of 60 leaf samples, consisting of reflectance spectra and leaf aphid density, was divided into two groups. Thirty-six leaf samples were selected randomly and used to calibrate the regression models, whilst the other twenty-four were used for validating the model. Correlation analysis was carried out to examine the sensitivity of each feature variable including spectral index and wavelet feature to aphid density. The sensitivity was described by the absolute coefficient of correlation (R^2) between the feature variables and aphid density. Higher absolute values of R indicate greater sensitivity of the feature. Coefficients of determination (R^2) and p value were derived from data analyses to evaluate models that corresponded to the calibration set. Based on the sensitivity analysis of the feature variables, a multivariate linear regression (MLR) analysis was applied for developing multivariate models for estimating aphid density. Two MLR models were established based on sensitive spectral indices and sensitive wavelet features, respectively. The predictive capabilities of the two MLR models were assessed based on the predictive R^2 value and the root mean square error (RMSE) between the measured and predicted aphid density. The formula of RMSE is:

$$RMSE = \sqrt{\frac{\sum_{i=1}^{n} (e_i - o_i)^2}{n}} \tag{3}$$

where n is the sample number, and e_i and o_i are the predicted and measured values of the model, respectively.

Results and discussion

Response of leaf reflectance to aphid density

Figure 1 shows the aphid-infested leaf spectrum (average spectrum of sample leaves with aphid density >80) and non-infested leaf spectrum (average spectrum of sample leaves with aphid density <5). It was easy to see that the reflectance of the leaf infested by aphid was higher in the visible (VIS) region and short-wave infrared (SWIR) region, but lower in

the near-infrared (NIR) region than the reflectance of the non-infested leaf. It has been reported that leaf optical properties are a function of the plant internal and external structure, water content and biochemical concentration (Jacquemoud et al. 1996; Gitelson et al. 2002; Sims and Gamon 2002). The leaf spectra were mainly influenced by pigment concentrations in the VIS region and the leaf internal structure in the SWIR region. In the SWIR region, the spectra were dominated by leaf water absorption and had the greatest sensitivity to water content (Carter 1991; Riedell and Blackmer 1999). Aphid feeding by piercing the leaf and sucking out leaf juice caused a reduction in pigment concentrations especially chlorophylls and leaf water content in the infested leaf and therefore it exhibited a higher reflectance in the VIS and SWIR regions than the non-infested leaf. Also, infested leaf tissue was destroyed and multiple scattering became weaker (Riedell and Blackmer 1999; Graeff and Claupein 2007), leading to a lower reflectance than for the non-infested leaf in the NIR region.

It should be noted that the spectrometric measurements have been done only after aphids were removed from the sample leaves because aphid populations are highly mobile and tend to travel (e.g. from leaf to leaf, plant to plant) after an infestation or when the surrounding environment is no longer suitable for their survival. Therefore, it is obvious that for cropping fields under aphid attack, most leaves would appear to be in the "post-attack" status (i.e. no aphids on most leaves). For remote sensing observations at canopy level or at a larger scale, the spectral contribution from infested plants or leaves is dominant, compared with the signal from aphids themselves which have little effect on spectral characteristics. It may be concluded that the spectral analysis of the post-attacked leaves, as conducted in the present study, is meaningful for monitoring aphid attacks over large areas.

Correlation of spectral indices with leaf aphid density

A correlation analysis was carried out between the 14 spectral indices from Table 1 and aphid density, respectively. Table 2 summarises the results of the correlation analyses. The spectral indices that had a significant relationship with leaf aphid density (p value <0.0001) were DSSI1, PRI, AI, NBNDVI, SIPI and MCARI, whilst NDWI and NPCI were also correlated to leaf aphid density (p value <0.001). The other spectral indexes showed low or no correlation with aphid density.

Correlation scalogram for aphid density

Figure 2 shows a correlation scalogram for aphid density and spectral reflectance of leaf by continuous wavelet analysis. A squared correlation coefficient (R^2) was reported for each

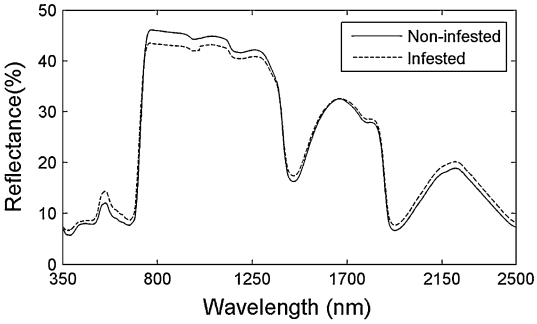

Fig. 1 Representative spectra of leaves non-infested and infested by aphid. (The average spectrum of sample leaves with aphid density more than 80 represents infested leaf spectrum, and the average spectrum of sample leaves with aphid density less than 5 represents non-infested leaf spectrum)

Table 2 Coefficient of determination between Spectral Index and aphid density (N = 36)

Spectral Index	R	R^2	*p* Value	Spectral Index	R	R^2	*p* Value
AI	−0.75	0.56	0.000	NBNDVI	−0.55	0.31	0.000
ARI	0.13	0.02	0.443	PSRI	0.32	0.10	0.054
DSSI1	0.61	0.37	0.000	SIPI	0.59	0.35	0.000
DSSI2	−0.23	0.05	0.179	MCARI	0.64	0.41	0.000
PRI	−0.57	0.33	0.000	PhRI	0.14	0.02	0.425
TVI	0.41	0.17	0.001	NPCI	0.42	0.18	0.001
NDWI	−0.53	0.28	0.001	NRI	0.35	0.12	0.036

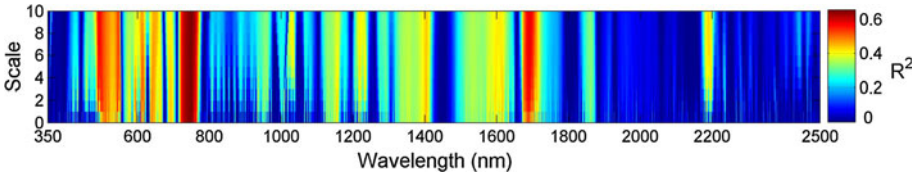

Fig. 2 Correlation scalogram relating wavelet power with aphid density in the calibration dataset (N = 36)

correlation scalogram at each wavelength and scale. The R^2 values were obtained for the linear correlation established between wavelet power and aphid density. Therefore, each element of the correlation scalogram represented a feature characterized by the R^2 value, wavelength and scale. The R^2 values ranged from 0 to 0.65.

Most informative wavelet features for estimating leaf aphid density

The most informative features for an independent variable were (1) retaining features where the correlations were statistically significant ($p < 0.0001$) and (2) to rank these features in descending order based on the R^2 values and to retain those encompassing the top 5 % (Fig. 3). Therefore, the cut-off R^2 value was determined as 0.48; when R^2 was more than 0.48 ($p < 0.0001$), we considered the wavelet feature ranges were sensitive to aphid density. The informative wavelet features were in the ranges of 484–552, 609–619, 637–651 718–770 and 1 673–1 713 nm in every scale (Fig. 2).

The maximum R^2 value in each wavelet feature range was selected, and the wavelength and scale of the five distinct wavelet features most strongly correlated with aphid density are shown Table 3. The low scale features (491 nm, scale 3), (617 nm, scale 3), (639 nm, scale 3), and (750 nm, scale 2) captured narrow absorption features that were primarily influenced by pigment concentration. High-scale (ranging from 6 to 10) features (1690 nm, scale 6) captured broad changes in strong water absorption. The R^2 value and *p* value showed that the most informative wavelet features performed better than spectral indices in estimating the leaf aphid density. The strongest relationship between leaf aphid density and wavelet power for an individual feature was located in scale 2 and at 750 nm. Because it was located in the red-edge range, it was concluded that the red edge might be the most sensitive to aphid density.

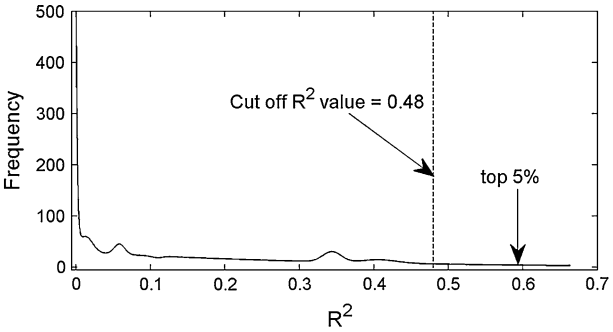

Fig. 3 Example of the frequency distribution of R^2 values observed for the scalogram in Fig. 2. The cut-off R^2 value used to delineate features correlated to aphid density

Table 3 Correlations between aphid density and most informative wavelet features derived from the calibration set

Feature code	Feature location		R	R^2	*p* Value
	Wavelength (nm)	Scale			
A	491	3	−0.76	0.58	0.000
B	617	3	0.73	0.53	0.000
C	639	3	0.70	0.49	0.000
D	750	2	0.81	0.66	0.000
F	1690	6	−0.76	0.58	0.000

Regression model for aphid density and validation

The MLR model 1 was constructed with the best six spectral indices including DSSI1, PRI, AI, NBNDVI, SIPI and MCARI, which were significantly correlated with aphid density (p value <0.0001), whilst the MLR model 2 was established with the most informative five wavelet features. The two MLR models were validated using the validation dataset, and the potential predictability of these models in estimating aphid density was assessed using the R^2 and RMSE values of the predicted and measured values. The results showed that the MLR model 2 ($R^2 = 0.72$, RMSE = 16.87) was better than the MLR model 1 ($R^2 = 0.56$, RMSE = 21.19) in estimating aphid density (Fig. 4). This result suggested that the spectral features extracted through CWT could approximately reflect aphid density.

Implications of wavelet features under field conditions

The results show that CWT as a spectral feature analysis tool has great potential for estimating aphid infestation density at leaf level in the laboratory. Laboratory analysis at the leaf level is the first step toward the goal of using remote sensing technology to detect aphid density in a wheat field. Based on this result, wavelet features and CWT could be used as a basis to further explore suitable spectral features for estimating aphid infestation density using hyperspectral data in the field, and specific sensors based on these efficient bands or spectral features for practical use may be developed in future. This capability would enable more precise targeting of pesticides on those places in the field where they are needed.

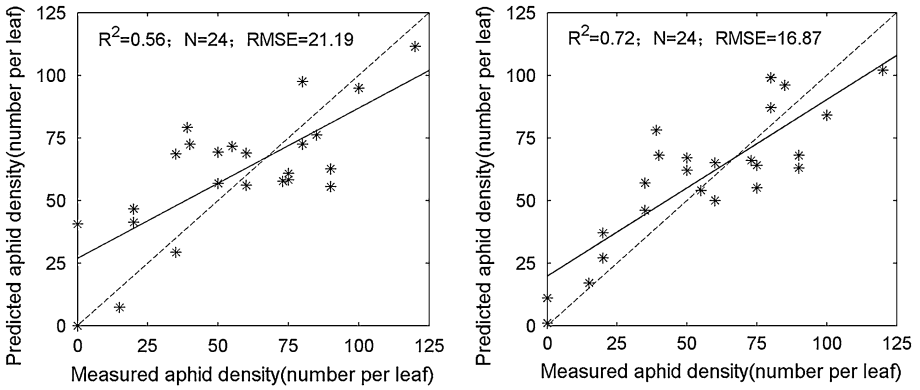

Fig. 4 Plots of measured versus predicted aphid density using MLR model 1 (*left*) and MLR model 2 (*right*). The predicted R^2 and RMSE values shown are obtained from the validation dataset. *Dashed lines* are 1:1 line

Conclusion

This work has tried to detect aphid infestation density using spectral response features of damaged leaves by aphid. The study has demonstrated the feasibility of applying CWT to leaf reflectance spectra in estimating aphid density. By decomposing the reflectance spectra into various scales, CWT can effectively identify meaningful spectral information relevant to aphid density. Five wavelet feature regions for aphid density were identified based on a threshold R^2 value ($R^2 = 0.48$). Study results showed that the five most informative wavelet features (one per feature region) extracted from the correlation scalogram were related to chlorophyll concentration, chlorophyll absorption, cellular structure, water content and dry matter. Among them, the wavelet feature (750 nm, scale 2) had the best correlation with aphid density ($R^2 = 0.66$). The correlation between spectral indices and aphid density showed a high correlation for DSSI1, PRI, AI, NBNDVI, SIPI and MCARI (p value <0.0001).Two MLR models had been established based on the six spectral indices and the five most informative wavelet features, respectively. The validation result confirmed that the MLR model using wavelet features was better in estimating aphid density than the MLR model based on spectral indices.

The study demonstrated that CWT was an effective method to extract the sensitive wavelet features from hyperspectral data to aphid density and to estimate aphid density at leaf level. In future, it will be necessary to test the capability of CWT to estimate aphid damage and aphid density at canopy/field level with onboard hyperspectral images.

Acknowledgments This work was subsidized by Hundred Talent Program of the Chinese Academy of Sciences of Wenjiang Huang, Beijing Municipal Natural Science Foundation (4122032), National Natural Science Foundation of China (41101395), National Key Technology R&D Program (2012BAH29B02). The authors are grateful to Mr. Weiguo Li, and Mrs. Hong Chang for data collection.

References

Ahmed, N. E., Kanan, H. O., Inanaga, S., Ma, Y. Q., & Sugimoto, Y. (2001). Impact of pesticide seed treatments on aphid control and yield of wheat in the Sudan. *Crop Protection, 20*, 929–934.

Ayala-Silva, T., & Beyl, C. A. (2005). Changes in spectral reflectance of wheat leaves in response to specific macronutrient deficiency. *Advances in Space Research, 35*, 305–317.

Blackburn, G. A. (2007). Wavelet decomposition of hyperspectral data: a novel approach to quantifying pigment concentrations in vegetation. *International Journal of Remote Sensing, 28*, 2831–2855.

Blackburn, G. A., & Ferwerda, J. G. (2008). Retrieval of chlorophyll concentration from leaf reflectance spectra using wavelet analysis. *Remote Sensing of Environment, 112*, 1614–1632.

Broge, N. H., & Leblanc, E. (2001). Comparing prediction power and stability of broadband and hyperspectral vegetation indices for estimation of green leaf area index and canopy chlorophyll density. *Remote Sensing of Environment, 76*, 156–172.

Broge, N. H., & Mortensen, J. V. (2002). Deriving green crop area index and canopy chlorophyll density of winter wheat from spectral reflectance data. *Remote Sensing of Environment, 81*, 45–57.

Carter, G. A. (1991). Primary and secondary effects of water content on the spectral reflectance of leaves. *American Journal of Botany, 78*, 916–942.

Cheng, T., Rivard, B., & Sánchez-Azofeifa, A. (2011). Spectroscopic determination of leaf water content using continuous wavelet analysis. *Remote Sensing of Environment, 115*, 659–670.

Cheng, T., Rivard, B., Sánchez-Azofeifa, G. A., Feng, J., & Calvo-Polanco, M. (2010). Continuous wavelet analysis for the detection of green attack due to mountain pine beetle infestation. *Remote Sensing of Environment, 114*, 899–910.

Daughtry, C. S. T., Walthall, C. L., Kim, M. S., Brown de Colstoun, E., & McMurtrey, J. E. (2000). Estimating corn leaf chlorophyll concentration from leaf and canopy reflectance. *Remote Sensing of Environment, 74*, 229–239.

Filella, I., Serrano, L., Serra, J., & Penuelas, J. (1995). Evaluating wheat nitrogen status with canopy reflectance indices and discriminant analysis. *Crop Science, 35*, 1400–1405.

Fluckiger, C. R., Kristinsson, H., Senn, R., Rindlisbacher, A., & Beholder, H. G. V. (1992). CGA-215944—a novel agent to control aphids and whiteflies. *Proceedings of the Brighton Crop Protection Conference*, British Crop Protection Council, Alton. pp 43–50.

Gamon, J. A., Serrano, L., & Surfus, J. S. (1997). The photochemical reflectance index: an optical indicator of photosynthetic radiation use efficiency across species, functional types and nutrient levels. *Oecologia, 112*, 492–501.

Gao, B. C. (1996). NDWI—A normalized difference water index for remote sensing of vegetation liquid water from space. *Remote Sensing of Environment, 58*, 257–266.

Gitelson, A. A., Merzlyak, M. N., & Chivkunova, O. B. (2001). Optical properties and nondestructive estimation of anthocyanin content in plant leaves. *Photochemistry and Photobiology, 74*, 38–45.

Gitelson, A. A., Zur, Y., Chivkunova, O. B., & Merzlyak, M. N. (2002). Assessing carotenoid content in plant leaves with reflectance spectroscopy. *Photochemistry and Photobiology, 75*, 272–281.

Graeff, S., & Claupein, W. (2007). Identification and discrimination of water stress in wheat leaves (*Triticum aestivum* L.) by means of reflectance measurements. *Irrigation Science, 26*, 61–70.

Halbert, S. E., Connelly, B. J., Bishop, G. W., & Blackmer, J. L. (1992). Transmission of barley yellow dwarf virus by field collected aphids (Homoptera: Aphididae) and their relative importance in barley yellow dwarf epidemiology in southwestern Idaho. *Annals of Applied Biology, 121*, 105–121.

Higley, L. G., & Pedigo, L. P. (1993). Economic injury level concepts and their use in sustaining environmental quality. *Agriculture, Ecosystems & Environment, 46*, 233–243.

Jacquemoud, S., Ustin, S. L., Verdebout, J., Schmuck, G., Andreoli, G., & Hosgood, B. (1996). Estimating leaf biochemistry using the prospect leaf optical properties model. *Remote Sensing of Environment, 56*, 194–202.

Larsson, H. (2005). A crop loss model and economic thresholds for the grain aphid, *Sitobion avenae* (F.), in winter wheat in southern Sweden. *Crop Protection, 24*, 397–405.

Luo, J. H., Huang, M. Y., Zhao, J. L., Huang, W. J., & Zhang, J. C. (2011). Spectrum characteristics of winter wheat infected by aphid in filling stage. *Transactions of the Chinese Society of Agriculture Engineering, 27*, 215–219. (in Chineses).

Lyda, S. D., & Burnett, E. (1970). Influence of benzimidazole fungicides on phymatotrichum omnivorum and phymatotrichum root rot of cotton. *Phytopathology, 60*, 726–728.

Mallat, S. (1991). Zero-crossings of a wavelet transform. *IEEE Transactions on Information Theory, 37*, 1019–1033.

Merzlyak, M. N., Gitelson, A. A., Chivkunova, O. B., & Rakitin, V. Y. (1999). Non-destructive optical detection of leaf senescence and fruit ripening. *Physiology Plantarum, 106*, 135–141.

Mirik, M., Michels, G. J., Kassymzhanova-Mirik, S., & Elliott, N. C. (2006a). Spectral sensing of aphid (Hemiptera: Aphididae) density using field spectrometry and radiometry. *Turkish Journal of Agriculture and Forestry, 30*, 421–428.

Mirik, M., Michels, G. J, Jr, Kassymzhanova-Mirik, S., & Elliott, N. C. (2007). Reflectance characteristics of Russian wheat aphid (Hemiptera: Aphididae) stress and abundance in winter wheat. *Computers and Electronics in Agriculture, 57*, 123–134.

Mirik, M., Michels, G. J, Jr, Kassymzhanova-Mirik, S., Elliott, N. C., Catana, V., Jones, D. B., et al. (2006b). Using digital image analysis and spectral reflectance data to quantify damage by greenbug (Hemiptera: Aphididae) in winter wheat. *Computers and Electronics in Agriculture, 5*, 86–98.

Muraki, S. (1995). Multiscale volume representation by a DOG wavelet. *IEEE Transactions on Visualization and Computer Graphics, 1*, 109–116.

Peñuelas, J., & Inoue, Y. (1999). Reflectance indices indicative of changes in water and pigment contents of peanut and wheat leaves. *Photosynthetica, 36*, 355–360.

Pike, K. S., Reed, G. L., Graf, G. T., & Allison, D. (1993). Compatibility of imidacloprid with fungicides as a seed-treatment control of Russian wheat aphid and effect on germination, growth, and yield of wheat and barley. *Journal of Economic Entomology, 86*, 586–593.

Pimentel, D. (1995). Amounts of pesticides reaching target pests: environmental impacts and ethics. *Journal of Agricultural and Environmental Ethics, 8*, 17–29.

Rabbinge, R., Drees, E. M., Verberne, F. C. M., & Wesselo, A. (1981). Damage effects of cereal aphids in wheat. *European Journal of Plant Pathology, 87*, 217–232.

Riedell, W. E., & Blackmer, T. M. (1999). Leaf reflectance spectra of cereal aphid-damaged wheat. *Crop Science, 39*, 1835–1840.

Rivard, B., Feng, J., Gallie, A., & Sanchez-Azofeifa, A. (2008). Continuous wavelets for the improved use of spectral libraries and hyperspectral data. *Remote Sensing of Environment, 112*, 2850–2862.

Rush, C. M., & Lyda, S. D. (1982). The effects of anhydrous ammonia on membrane stability of phymatotrichum omnivorum. *Mycopathologia, 79*, 147–152.

Shaoyou, L., Stoltz, R. L., & Xinzhi, N. (1986). Damage to wheat by *Macrosiphum avenae* (F.) (Homoptera: Aphididae) in northwest China. *Journal of Economic Entomology, 79*, 1688–1691.

Sims, D. A., & Gamon, J. A. (2002). Relationships between leaf pigment content and spectral reflectance across a wide range of species, leaf structures and developmental stages. *Remote Sensing of Environment, 81*, 337–354.

Thenkabail, P. S., Smith, R. B., & Pauw, E. D. (2000). Hyperspectral vegetation indices and their relationships with agricultural crop characteristics. *Remote Sensing of Environment, 71*, 158–182.

Torrence, C., & Compo, G. P. (1998). A practical guide to wavelet analysis. *Bulletin of the American Meteorological Society, 79*, 61–78.

Whitson, R. S., & Hine, R. B. (1986). Activity of propiconazole and other sterol-inhibiting fungicides against phymatotrichum omnivorum. *Plant Disease, 70*, 130–133.

Yang, Z., Rao, M. N., Elliott, N. C., Kindler, S. D., & Popham, T. W. (2005). Using ground-based multispectral radiometry to detect stress in wheat caused by greenbug (Homoptera: Aphididae) infestation. *Computers and Electronics in Agriculture, 47*, 121–135.

Yang, Z., Rao, M. N., Elliott, N. C., Kindler, S. D., & Popham, T. W. (2009). Differentiating stress induced by greenbugs and Russian wheat aphid in wheat using remote sensing. *Computers and Electronics in Agriculture, 67*, 64–70.

Zhang, M., Qin, Z., Liu, X., & Ustin, S. (2003). Detection of stress in tomatoes induced by late blight disease in California, USA, using hyperspectral remote sensing. *International Journal of Applied Earth Observation and Geoinformation, 4*, 295–310.